# AN ABSTRACT OF THE THESIS OF

Amritha Ajithkumar for the degree of Master of Science in Electrical and Computer Engineering presented on December 5, 2018.

Title: Printed Nanocomposite Devices and Flexible Electronics for Humidity Sensing.

Abstract approved: _____
Li-Jing Cheng

The thesis focuses on the development of a novel printed resistive humidity sensor and integrated flexible electronics for an RFID-enabled humidity sensing platform. We explored a hybrid nanocomposite material for humidity sensing consisting of carbon nanomaterials, conductive polymer and cellulose polymer that undergoes resistance change in response to humidity change. The effects of material composition ratios, choice of material, and sensor dimension on sensing performance were investigated to achieve an optimal humidity sensitivity of about 0.02646 $\Delta R/R/\%RH$ (13.23 $\Omega/\%RH$) and a linearity correlation ($R^2$) of 0.96. We also demonstrated a wireless sensing platform by integrating the humidity sensor and an active UHF RFID on a flexible substrate all fabricated by screen printing technology. The sensing materials and printed flexible electronics integration developed in this study form the technical foundation of the future wearable sensing technology.

# Printed Nanocomposite Devices and Flexible Electronics for Humidity Sensing

by

Amritha Ajithkumar

A THESIS

submitted to

Oregon State University

in partial fulfillment of
the requirements for the
degree of

Master of Science

Presented December 5, 2018
Commencement June 2019

Master of Science thesis of Amritha Ajithkumar presented on December 5, 2018

APPROVED:

---

Major Professor, representing Electrical and Computer Engineering

---

Head of the School of Electrical Engineering and Computer Science

---

Dean of the Graduate School

I understand that my thesis will become part of the permanent collection of Oregon State University libraries. My signature below authorizes release of my thesis to any reader upon request.

---

Amritha Ajithkumar, Author

# ACKNOWLEDGEMENTS

I would like to express deepest gratitude to my advisor Dr. Larry Cheng for his expert guidance and encouragement throughout research. In addition, I express my appreciation to Dr. Leonard Coop, Dr. Matthew Johnston, and Dr. John Labram for having served on my committee. Their thoughtful questions and comments were valued greatly.

Thanks to everyone in the Dr Cheng Group, especially Bo and Ye without whom this work would not have taken flight. I treasure our impromptu discussions and the major opportunity on cultural exchange.

Thanks to my parents, my brother, all my near and dear friends.

Finally, I am ever grateful to my husband, Arun, for his unconditional love and sacrifices he endured during the last two years; this would not have been possible if not for his staunch belief in me.

# TABLE OF CONTENTS

Page

# LIST OF FIGURES

# LIST OF FIGURES (contd..)

# LIST OF TABLES

DEDICATION

To Leela, my grandmother.
She was and will always be my inspiration.

# 1. Introduction

Technology has quietly yet surely made inroads into our everyday life through integration of sensors promised by the rise of Internet of Things (IoT). It is printed electronics, as detailed in Kirchmeyer et al. [1] a guidepost to interlinked technologies, which holds the key to this rise. They are now popular for a wide range of applications such as large-area electronics, robotics, smart textiles and flexible electronics [2]. Printed electronics is created by printing processes, an additive technology that simplifies manufacturing processes, reduces material and process costs thereby allowing technology to be available across social strata cutting across inequities [3]. Wearable electronics have, in last few years, risen as an integral part of people's lifestyle. From heart rate sensor embedded within a watch on the wrist to medical applications, such as glucose measuring sensor over the hip or smart clothes – the reach of wearable printed electronics has transformed lives. On the same note, monitoring and real-time sensing of humidity could be applied to many applications and uses. For example, ambiance air quality could be set by monitoring and drawing patterns of breath moisture sensing. Allergens such as pollens and mites can be sanitized prior to health hazard from monitoring breath sensing. In this work, we report the development of printed nanocomposite-based humidity sensors and integration of printed RFID to demonstrate a wireless respiratory rate monitoring device in a wearable fashion.

## 1.1 Printed Humidity Sensing Technologies

Humidity sensing can be implemented through a variety of measuring principles such as capacitive, resistive, hygrometric, gravimetric, optical sensing. The following table compares state-of-the-art printed humidity sensors based on their (1) sensing technology, (2) sensing material, (3) substrate printed upon, (4) method of printing and (5) its performance.

Table 1.1 Table of comparison of previous work on printed humidity sensors.

| S.No | Ref. No | Material used | Substrate | Method of Printing | Sensing Technology | Sensitivity (del $R/R_o/\%RH$) | Responsivity |
|---|---|---|---|---|---|---|---|
| 1. | [4] | Carboxylate CNT ink | Paper | Inkjet printing | Capacitive | 2pF/RH% | Response time 4 to 5 min for 3 to 85%RH increase |
| 2. | [5] | Silver NP ink | paper | Inkjet printing | Resistive | 0.0124 * | ~15 min* |
| 3. | [6] | $TiO_2$ NP+ HPMC over gold layer | PET | Screen Printing | Resistive | $S\% = R_{ini} - R_{mes}/R_{ini}$ X 100; 80% response for 0 to 70% RH | Response time ~3min from 5 to 40%RH, Recovery time ~ 50s |
| 4. | [7] | CNT + CMC | Paper | Screen Printing | Resistive | 10 to 60% RH increases resistance by 15 times. | N/A |
| 5. | [8] | MWCNT/PEDOT: PSS | Polymer Kapton HN500 | Drop casting | Resistive | 0.070 | N/A |
| 6. | [9] | Graphene Oxide over piezoelectric ZnO thin film | Flexible Polyimide | Drop casting | Lamb wave frequency | 145.83 ppm/%RH at 85%RH | Absorption time ~ 20 s and Desorption ~ 5 s |
| 7. | [10] | Porous Silicon/ Ag IDE | Paper | Roll- to- roll (spray coating) | Resistive | 0.011* 500Mohm to 001Mohm for 0 to 90%RH | ~20 min* |
| 8. | [11] | MWCNT, P4VP, DBB on IDE Au electrode | Ceramic substrate | Automatic dip coating | Resistive | 470% increase from 1 to 30%RH | Response time ~265s, Recovery time ~ 152s |
| 9. | [12] | Ag NP Ink IDE with SL900a | PET | Gravure Printing | Resistive | Relative Sensitivity- Conductance at 80% RH at 70% | N/A |
| 10. | [13] | Polyaniline ink solution | Polyester Sheet | Inkjet Printing | Resistive | 0.0114* | Response time ~ 5 s |
| 11. | [14] | PEDOT:PSS, pHEMA, CAB and Nafion with Ag IDE | Kapton Polyimide sheet woven to textile | Inkjet Printing | Impedance | $10^7$ ohms to $10^4$ ohms from 60 to 100%RH | N/A |
| 12. | [15] | COOH -CNT | Cellulose Paper | Drop casting | Resistive | 0.00714* | Response time ~6s, Recovery time ~ 120s |
| 13. | [16] | Ag/MWCNT/Ag | Glass | Drop casting | Capacitive | Capacitance increases 366 times at 90RH | Response time ~2s, Recovery time ~ 8s |
| 14. | [17] | COOH- MWCNT, Au electrode | Quartz plate | Airbrush Spraying | Resistive | 0.0166* | Response time ~20s, Recovery time ~ 40s |
| 15. | [18] | Silver NP Ink | Kapton 500 HN Substrate | Inkjet Printing | Humidity dependent permittivity | 171.4kHz/%RH | N/A |
| 16. | [19] | Ag NP Ink | PET | Gravure Printing | Capacitive | 172% increase at 80%RH | N/A |
| 17. | [20] | Plasma-treated MWCNT/PI | Silicon nitride membrane | LPCVD | Resistive | 0.00466 | N/A |
| 18. | [21] | MWCNT | Stainless Steel | Drop Casting | Capacitive | 300% increase in capacitance response, 35.86%/RH% | Response time ~200s, Recovery time ~ 140s |

*Data extracted from the plots and graphs provided in each work.

Yoo et al. [20] reported a resistive-type humidity sensor based on a composite film consisting of carbon nanotube (CNT) and polyimide. In the polyimide water system, a decrease in resistance is detected in the presence of high conductivity of water. However, the sensor has a humidity sensitivity only of 0.0047 ΔR/R /%RH, a sensitivity insufficient for reliable data reading. In Jiang et al. [22] used MWCNT nests grown on arrayed nonporous silicon to show a relative change in resistance of up to 362% between 11% and 85 % RH. Its recovery and response time are however very long, reaching up to an hour each half cycle. Such a slow response makes it an unconvincing sensor for real-time measurement. Nanotube-enhanced capillary condensation for a capacitive humidity sensor is described in Yeow et al. [21] in which multi-walled carbon nanotubes (MWCNTs) within the CNT-enhanced sensor yield transduction change in response to varying water and air proportion due to the change in the effective dielectric of the sensing material. This reciprocates as change in capacitance that is proportional to the change in relative humidity. The small gap between CNT structures facilitates the condensation. The high-dielectric constant water causes a big change in the effective dielectric constant. However, the complicated manufacturing process inhibits the scalability of fabrication process and makes it difficult to integrate with a wearable device. Such limitations from previous works have limited the scope of its sensing capability and integration to wearables. There is a strong need for advanced sensor technology with improved performance and manufacturing methods.

## 1.2 Strategy of sensor creation

A variety of nanomaterials have been demonstrated for humidity sensings, such as semiconductor nanoparticles and carbon-based nanomaterials. Among them, carbon nanotubes (CNTs) have been a popular sensing material owing to its conductivity variable with environmental conditions, including charge, chemical, and moisture adsorption. CNTs are allotropes of carbon found in 1991 by Iijima et al., are 1D nanostructures with the whole weight dominated by their large surface structure. The large surface of tubulenes which determines the adsorption properties capable of highly sensitive chemical or humidity detection [8][24].

There are two common forms of CNTs - single-walled carbon nanotubes (SWCNTs) and multi-walled carbon nanotubes (MWCNTs), as shown in Figure 1. While SWCNTs are single surface carbon nanotubes with electronic properties varying with chirality [24], MWCNTs consist of multiple rolled layers of graphene and have an average effect of all chiral tubes. MWCNTs are more cost effective with higher molecular weight and better conductivity that have catapulted CNTs in a plethora of functionalities, such as in absorption and screening of electromagnetic waves, as additives to polymers and catalysts, composite materials (fillers or coatings), as nanoprobes, sensors, supercapacitors, etc.[17, 20].

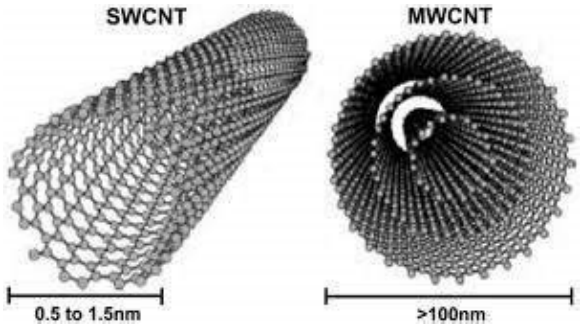


Figure 1. Structures of a single-walled carbon nanotube (SWCNT) and a multi-walled carbon nanotube (MWCNT)[23].

Looking into the humidity sensing aspect of CNTs, Zahab et al. [25] reported that p-type CNTswould turn into n-type after adsorption of water molecules. They demonstrated that the impedance of the CNT-based humidity sensor increases with increasing humidity. Cao et al. [17] explained in detail the humidity-dependent conductivity of MWCNTs. Humidity sensing using pristine CNT and doped CNTs described in Adjizian et al. [26] gives a full recovery of about 2.5 hours even when heated at 150$^{o}$C. A fast response of 30 s was reported in Yu et al. [27]. However, the impedance change of the composite between 5 and 85 % RH was not sensitive enough for the application. Li et al. [11] have reported humidity sensing based on the composite of multi-walled carbon nanotubes and cross-linked poly(4-vinylpyridine) (QC-P4VP) polyelectrolyte. It demonstrates the ability to detect humidity as low as 1%RH by exploiting the high intrinsic conductivity of MWCNTs; however, it has a slow recovery time. P4VP on its own has also been reported to have humidity sensing properties as in Liu et al. [28] but with a limited sensing dynamic range.

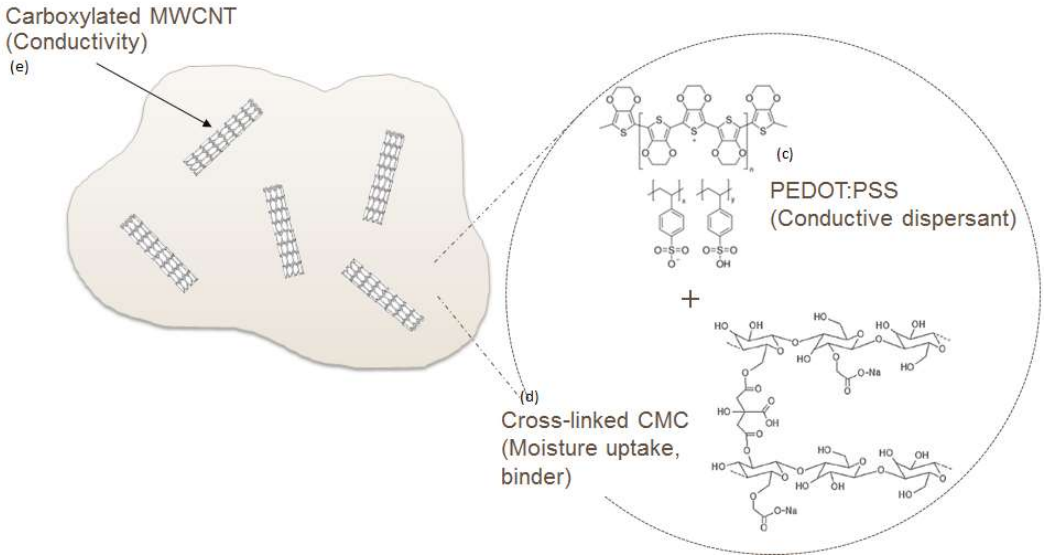


*Figure 2. (a) Schematic of C*NT-CMC-PEDOT:PSS ink composite. Structure of (b*) poly(3,4-ethylenedioxythiophene) polystyr*ene sulfonate (PEDOT:PSS), (c) *carboxymethylcellulose (CMC),* and(d*) carboxylate carbon nanotube (COOH-CNT).*[33]

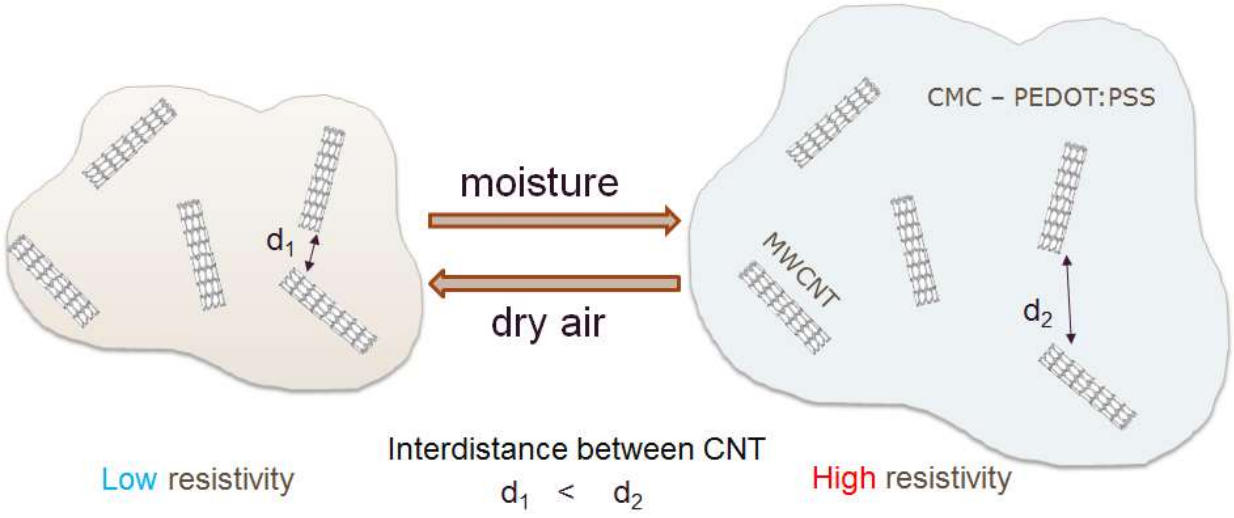


Figure 3. (e) Sensing mechanism of the humidity sensor.

In this work, we aim to develop an electrical humidity sensor with improved response speed and sensitivity. We develop a nanocomposite sensing material composed of CNT embedded polymer undergoes electrical conductivity change in response to the change in environmental moisture as

illustrated in Fig. 2(a). The nanocomposite contains poly (3,4-ethylenedioxythiophene) polystyrene sulfonate (PEDOT:PSS) (Fig. 2(c), crosslinked carboxymethyl cellulose (CMC) (Fig. 2(d)), and carboxylated MWCNTs (Fig. 2(e)). The nanocomposite utilizes CMC for reversible moisture uptake that induces slight volumetric expansion upon adsorption of moisture and shrinkage after evaporation. As depicted in Fig. 2(b), the volumetric change of CMC polymer further transduces the inter-CNT distance and therefore regulated the electrical conductivity of the nanocomposite. The sensing material can be applied and patterned on a flexible substrate using screen printing. From the literature review, we deduced that to prepare a screen-printable ink for sensor fabrication, a reliable binder and a dispersant are required along with the conductive MWCNT. We chose CMC as the binder and PEDOT:PSS as the conductive surfactant to aid in dispersion of CMC and MWCNT. CMC acts as a binder to improve the electrochemical property of ink as is explored in Barras et al. [7] where it was used with carbon fibers (CFs) within the purview of printable cellulose-based electro conductive composites for sensing elements in paper electronics. In addition, CMC crosslinks through its abundant carboxyl groups after heating that further strengthens the mechanical property of the sensor. We also use carboxylated MWCNT as opposed to pristine MWCNT to improve the dispersion property in preparing aqueous ink solutions as reported in David et al. [34].

PEDOT:PSS has been explored to improve electrical conductivity [8,14,20,31], aid in dispersion of CMC and CNT and in making ink with high ductility to feature in flexible wearable printable electronics.

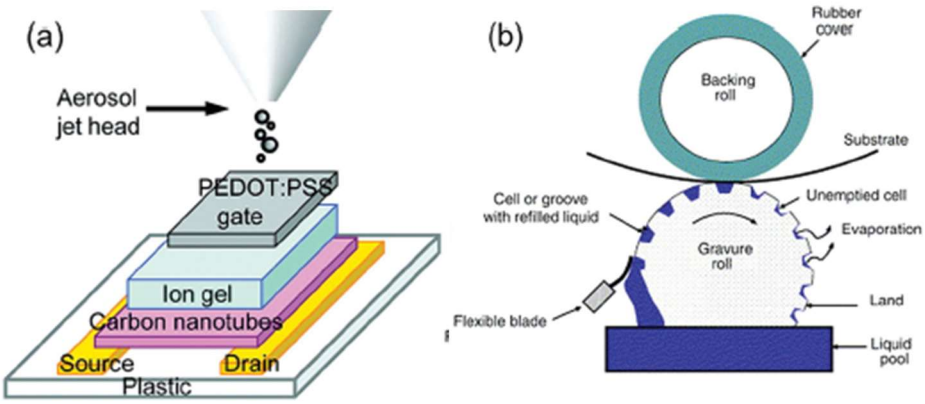


Figure 4. (a) inkjet printing, [3] and (b) gravure printing. [3]

A variety of printing technologies were attempted to transfer conductive inks based on metal nanoparticles, carbon nanotubes, and graphene, for printed electronics. The printing technologies include inkjet printing (Fig 3(a)), spin-coating, drop-casting, screen printing, direct ink printing, and gravure printing (Fig 3(b)). [36, 37]We tested printing via inkjet, ballpoint, pipette- drop, spin coating. Screen printing[17][39] was adopted for creating flexible sensors and circuit boards. Screen printing provides the capability of large-area manufacturing, cost-effect process, and spatial resolution sufficient our applications.

Apart from printing techniques, we also explored flexible and tactile substrates for the printed electronics. Sicong et al. [28] reported patterning of flexible and conductive material on a cotton fabric via inkjet printing under ambient conditions. Zhang et al. [38] demonstrated CNT-based and graphene-based hybrid films fabricated on arbitrary substrates or surfaces such as perforated polyethylene terephthalate (PET) substrates. After multiple printing tests using our nanocomposite ink on a spectrum of substrates, including glass, nylon net filters (NY41, EMD Millipore), and PET (50 um thick), we chose PET for its flexibility, transparency, and its adaptability to withstand 150oC heat treatment required for the ink curing process.

## 1.3 Inspiration and Research Goals

IoT and wearables[40, 41] are the need of the hour for a more fit and able lifestyle. Our main goal is to fabricate and characterize a new type of printed humidity sensor and integrate with a printed RFID in a wearable fashion to demonstrate real-time respiratory rate monitoring [18]. We will also investigate the effect of dimension and composition of the sensor on the sensitivity and pace of change [19-22]. An ideal sensor would traverse a larger gradient of magnitude in the shortest time possible. A sensor with high responsivity and sensitivity for reliable sensing was our main aim. We are also looking to integrate with RFID for continuous real-time data logging.

# 2 Experimental

## 2.1 Chemical and Materials

Commercially available carboxylated MWCNTs obtained from US Research Nanomaterials, Inc were used in this experiment. The COOH-functionalized MWCNT were 5-15 µm in length with purity above 95%. The hydrophilicity of the MWCNTs rendered by the carboxylate functional groups improves their dispersion in aqueous solutions and increases the adhesion with the substrate printed upon [15]. Sodium carboxymethyl cellulose (CMC) m.w. 90,000 and poly (3,4-ethylenedioxythiophene)-poly (styrene sulfonate) (conductive grade PEDOT:PSS) 1.3 wt.% dispersion in $H_2O$ were obtained from Sigma-Aldrich Dupont Silver Ink PE 873-4 with purity over 95% was used for fabricating screen-printed electrodes and RFID circuits. All the chemicals used in the work were of analytical grade and used as received unless noted otherwise.

## 2.2 CNT Ink Preparation

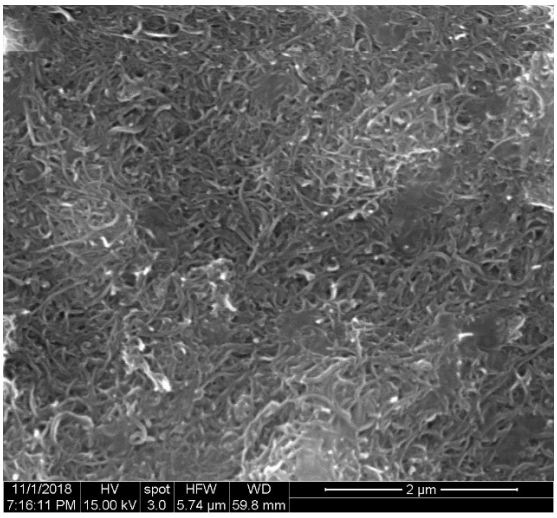


Figure 5. SEM image of the cured nanocomposite ink consisting of CNT, CMC, and PEDOT:PSS.

PEDOT:PSS (0.2 wt.%) was uniformly dispersed in DI water with 30 mg/ml CMC. This mixture was heated to 60$^{o}$C for 10 minutes to aid uniform dispersion of CMC in water. Once well dispersed, 30 mg/ml carboxylated MWCNT was added. Repeated sonication and vortex (2 minutes for each) for a total of 30 minutes was performed to prevent settling of heavy CNT particles and aid uniform distribution. Probe sonication was carried out for 10 minutes at 20% amplitude and 2 second pulse width. To prevent evaporation, probe sonic was used for a minute at a time and altered between vortex and ultrasonic treatment. The ink requires a viscosity fit for screen printing. Fig. 4 shows an SEM image of CNT nanocomposite ink after 150$^{o}$C curing.

## 2.3 Device Fabrication

A sensor device pattern (0.5 mm width and 8 mm length), an interdigitated electrode (IDE) (0.4 mm width, 10 mm length) was created using Inkscape and printed on transparent sheets using a laser printer. Figures 5(a), 5(b) and 5(c) show the layouts of IDE, sensor, and RFID circuit, respectively. The patterns were created on stencil masks using pre-emulsified mesh silk screen printing sheets (EZScreenPrint).

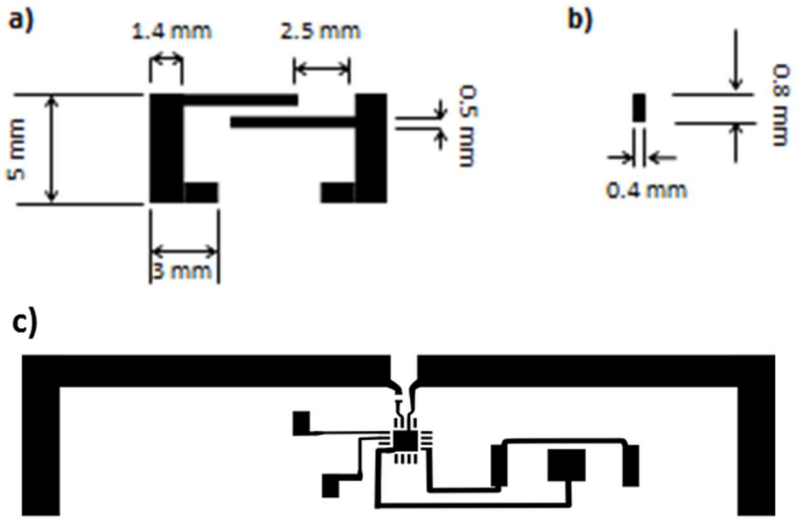


Figure 6, Layouts of (a) interdigitated electrode (IDE), (b) sensor pattern, and (c) AMS SL900a RFID circuit. [49]

Each stencil was made by UV lithographic transfer of the layout designs from the transparent sheet to a screen mask. Using a black felt board and a glass, the mask was clasped on either side with the stencıl on it and exposed to UV light (Fig. 6(a)). This was done to prevent seeping of UV away from the pattern that causes blurring of the pattern on the stencil. The optimal UV exposure times are 6 minutes for IDE and sensor layouts and 8 minutes for the RFID circuit layout. After UV exposure, the stencil was left in warm water for 20 minutes, dried, and then exposed to UV light once again for 10 minutes. After patted dry and left to harden at room temperature, the stencil as shown in Fig. 6(b) is ready for screen printing process.

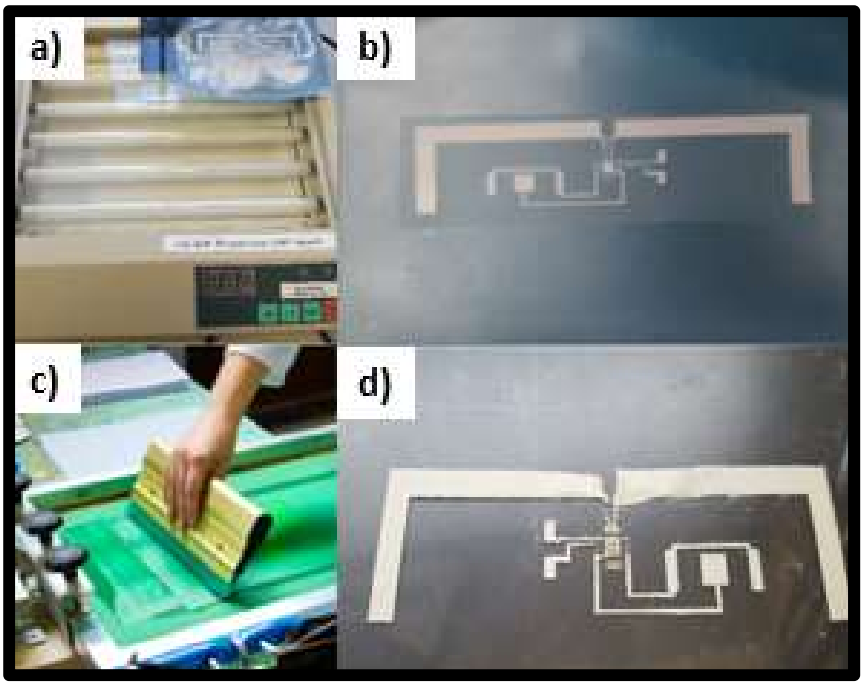


Figure 7. (a) UV exposure box. (b) Stencil mask. (c) Screen printing technique [48]. (d) Screen printed RFID circuit using silver ink on a PET film.

To start the screen printing process as shown in Fig. 6(c), the mask stencil was secured on a frame, placed over the PET, and clasped down to prevent seepage of ink off the pattern. To improve the adhesion of the printed silver ink and CNT ink on the PET surface, the PET thin film was first treated with oxygen plasma to obtain a hydrophilic surface.t. A rubber squeegee was used to apply ink through the stencil and remove the excess ink off the pattern. The frame with the stencil was gently lifted to reveal the screen-printed pattern on the PET. The humidity sensor was fabricated by a two-step screen printing process. The CNT nanocomposite pattern was first printed on PET and crosslinked at 150ºC for 1.5 hr. The substrate was kept flattened during thermal treatment by clamped between two glass slides. Silver electrode patterns were then printed using silver ink PE874 (Dupont) followed by 160ºC curing for 10 minutes. The process resulted in a bottom CNT

sensor layer covered by the Ag IDE pattern as shown in Fig. 7(a). Fig. 7(b) and 7(c) show the SEM images of the sensor area with both left and right sides covered by Ag electrodes. The SEM image in Fig. 7(c) resolves the boundary of the Ag electrode and sensor area.

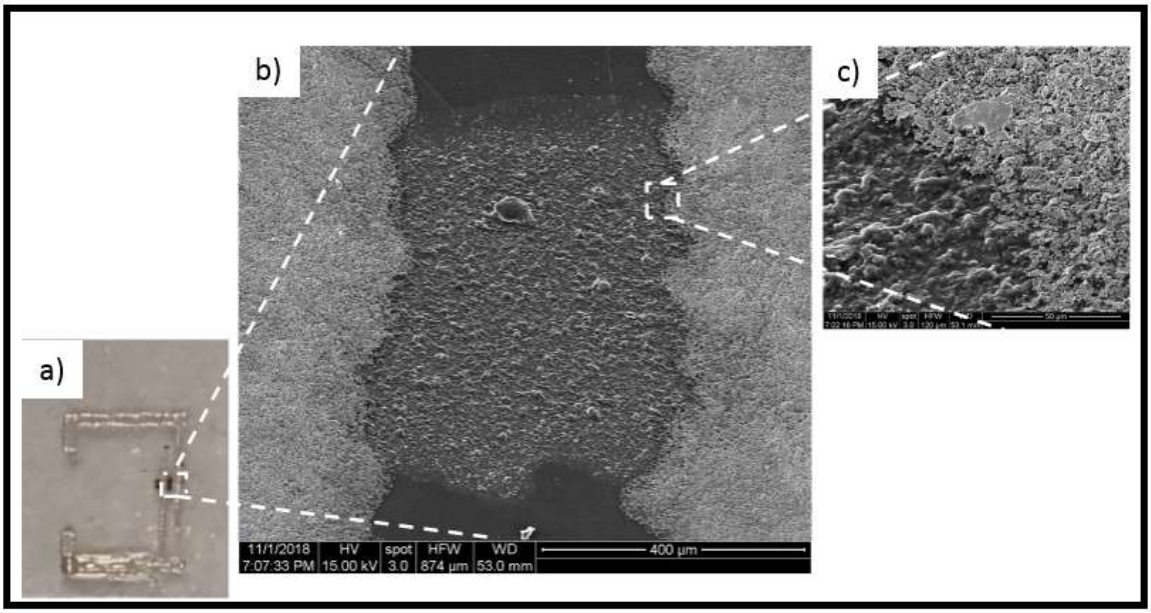


Figure 8. (a) Image of the printed humidity sensor, (b) Top-view SEM image of the printed sensor bounded by Ag electrodes on either side. (c) SEM image of the boundary between silver electrode and sensor area.

The sensor was electrically connected to the characterization tool through copper strips attachea d to the sensor electrodes using silver paste, and the junctions were secured by UV-curable adhesive to obtain high reliability.

## 2.4 Characterization Set Up

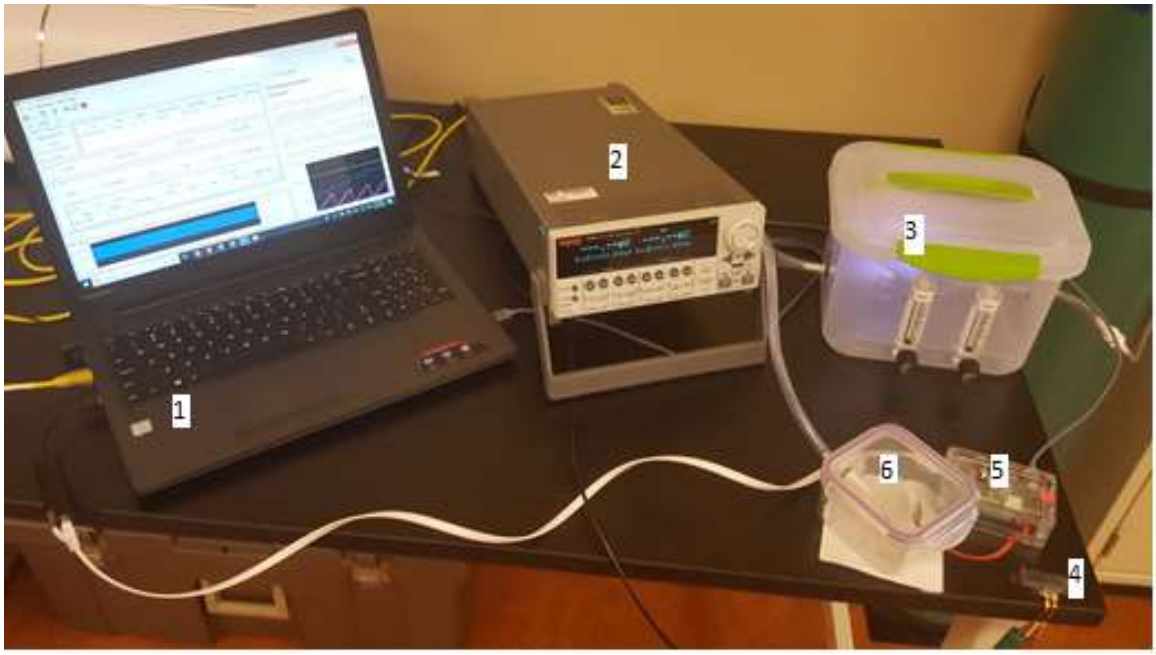


Figure 9. Characterization setup including (1) a laptop, (2) Keithley 2636B Sourcemeter, (3) humidity creation chamber, (4) device under test (DUT), (5) Raspberry Pi humidity sensor, and (6) humidity test chamber.

The electrical resistance of the humidity sensor was characterized using a KEITHLEY electrometer as shown in Fig. 9 under various humidity conditions varying from 10 to 99% RH. The humidity levels inside the closed chamber were controlled by a home-made humidity generation system [3] that regulates the inflow air humidity by mixing dry air (dry $N_2$) and humidified air with controllable ratios. The system was maintained at room temperature. [19]

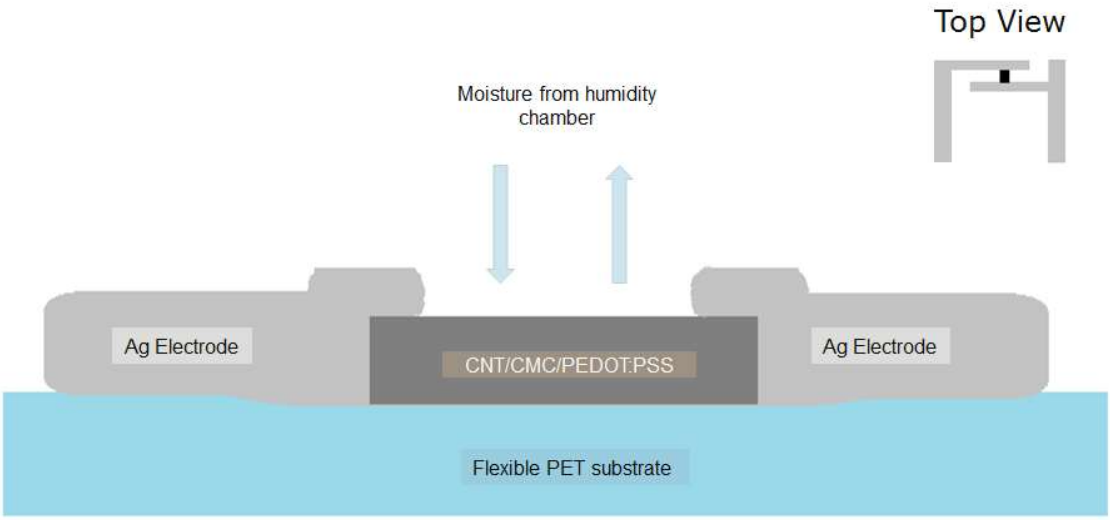


Figure 10. Schematic of the humidity sensor under test.

# 3 Result and Discussion

## 3.1 Characterization Result of Humidity Sensing

The humidity sensor was characterized using the setup in Fig. 8. The flow rate was kept constant to achieve a constant humidity. The resistance of the sensor was measured under a constant humidity level to analyze the sensitivity. We also monitored the resistance change in response to a rapid humidity change to evaluate the response speed of the sensor. Overall, the resistance of the humidity sensor increases as the environmental humidity increases. The trend agrees with the sensing mechanism explained in the previous section. The randomly distributed MWCNT network increases further in the inter-particle distance on the absorption of moisture by CMC. Therefore, the increase in humidity raises the resistance of the device. Fig. 10 shows the responsivity of the sensor in low humidity range. The sensor exhibits a short 1 second fall time as the relative humidity drops from 36% to 9% and takes about 30 seconds to recover when the humidity returns to 36%. Figures 11, 12 and 13 show the sensing characterization of the sensor in the lower humidity range. The results suggest a historical effect on the sensor during recovery periods. The starting resistance increases with the increase of the humidity variation cycles; however, the resistance measured at low humidity levels remain consistent. The other notable observation is that from 9% RH to 20% RH, the fall time is within a second, however, in the range between 24% RH to 33% RH, the fall time becomes comparable to it rise time. There was no observable sensing between the ranges 33% RH to 49% RH. Figures 14 and 15 show us a glimpse of sensor characteristics in higher humidity range. The resistance increases with the absorption of moisture and quickly recovers once exposed back to room humidity. The rate of resistance change is accelerated when exposed to a relatively higher humidity level. These observations suggest that the property would lead to

a reliable respiratory rate monitor sensor, which traces breathing rate through the moisture variation induced by exhalation and inhalation.

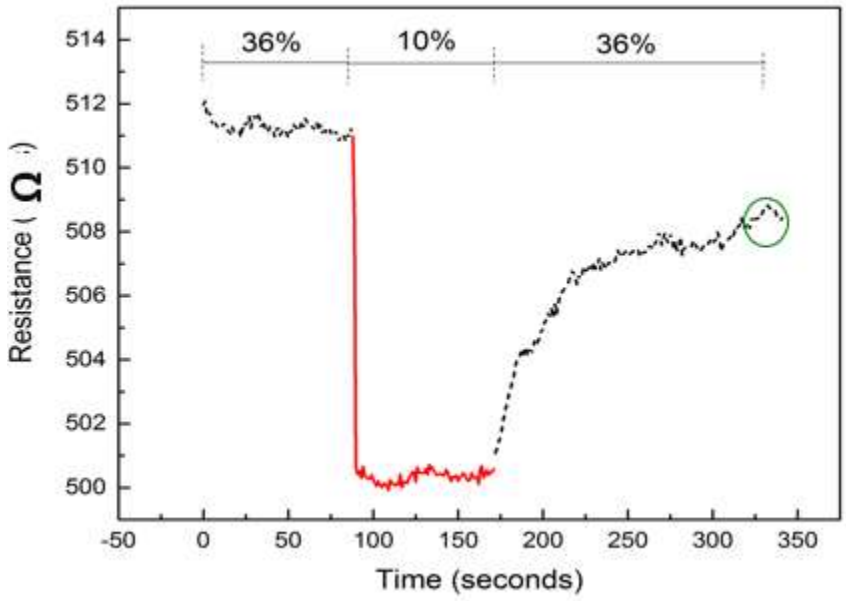


Figure 11. Change in the measured resistance of the sensor at 0.5V as RH was switched between 10% RH and 36% RH.

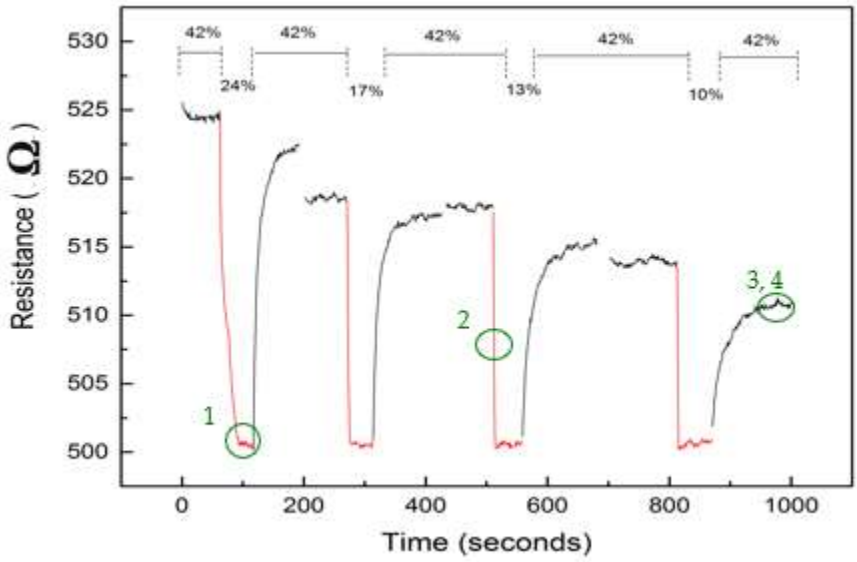


Figure 12. Resistive response between 42%RH and different %RH.

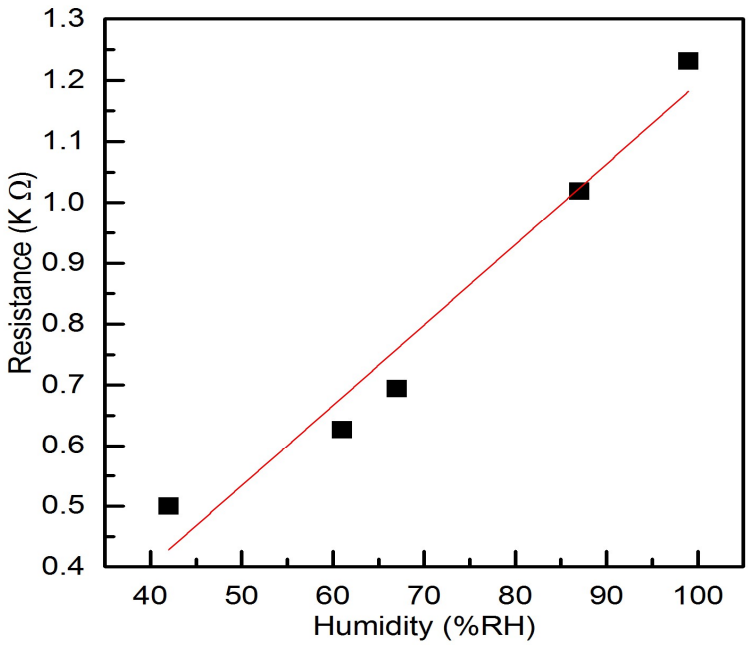


Figure 13. Calibration curve of humidity sensor.

Sensing characteristic of a humidity sensor with 5 electrode pair IDE (Fig 14 c) is shown in Fig 13 and Fig. 15(c). The sensor layer was printed over the Ag IDE initially to evaluate the sensing performance. The fastest sensing response occurs at a high humidity level of 90 %RH, yielding a 40 second rise time and about 9 second fall time. The reading of the sensor was taken when the humidity chamber was stabilized on a given relative humidity. During this condition, the flow rate was kept constant to minimize the effect of flow rate. Fig. 17 shows the sensitivity of the sensor at different humidity levels. This shows that the sensor could be a point to point reference of resistance for a given humidity in the higher humidity range.

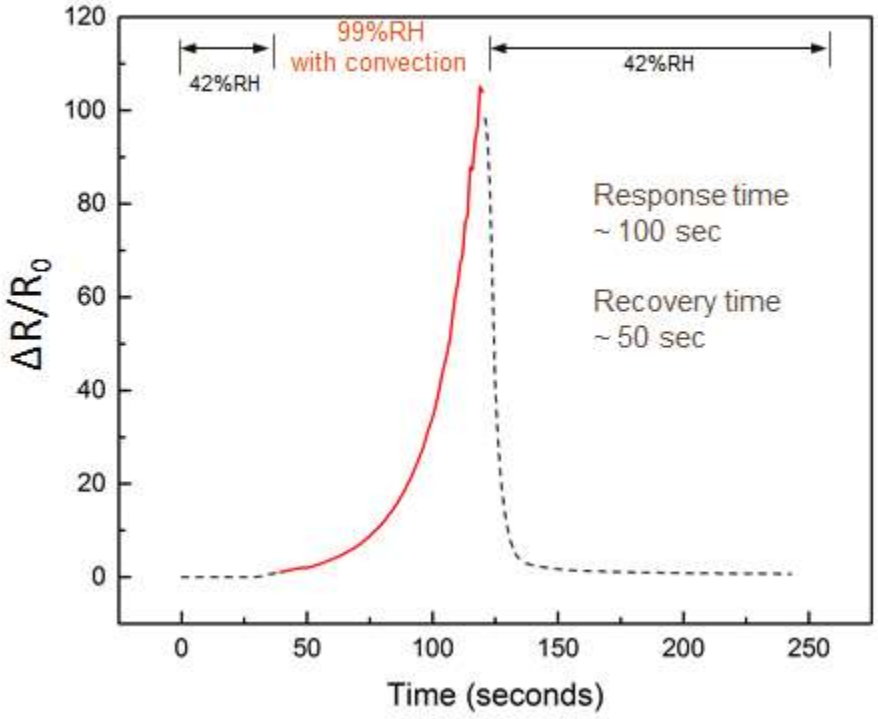


Figure 14. Responsivity of the sensor in response to rapid humidity change between 42% RH and 99% RH.

3.2 Optimization of Humidity Sensing

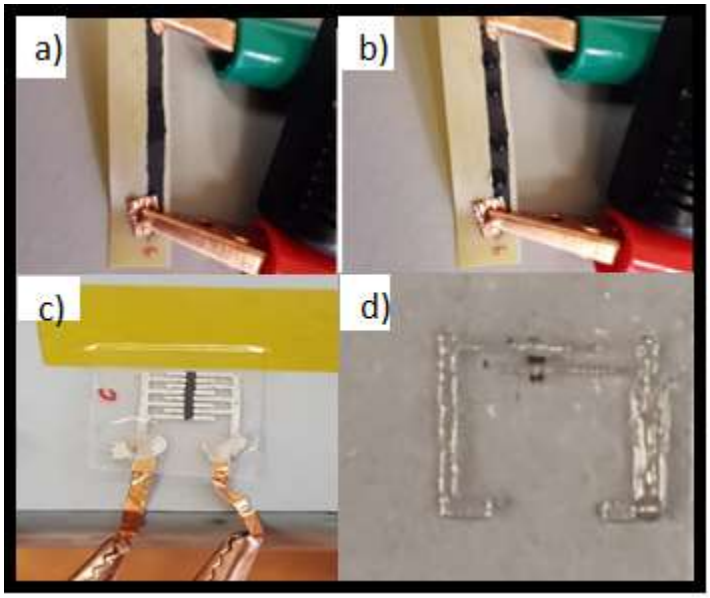


Figure 15. Humidity sensors with various device configurations for performance optimization. Large-dimension sensor printed on nylon mesh (a) under dry condition, and (b) during wet sensing test. (c) Five-electrode pairs IDE with a top sensing layer, and (d) single electrode pair IDE with a bottom sensing layer screen printed on PET.

The dimension of the humidity sensor was found to affect its sensitivity and responsivity. Figure 14.(a) and 18(b) are large-area sensors (3 cm length and 0.5 cm width) originally designed for wet sensing. The bulky, large-area device yielded long response and recovery time in response to humidity change making it not suitable for our application. We ascribe the slow response to the large sensing volume that requires more time to uptake enough moisture to produce observable resistance change. Based on the rationale, the sensor was reduced using IDE structure to improve the response of the sensor as shown in Fig. 18(c) and 18(d). The sensing area can be further scaled

down to 0.8 mm x 0.4 mm by covering part of it with a silver IDE printed on its top. The reduced size of the sensor showed a remarkable improvement in sensing responsivity.

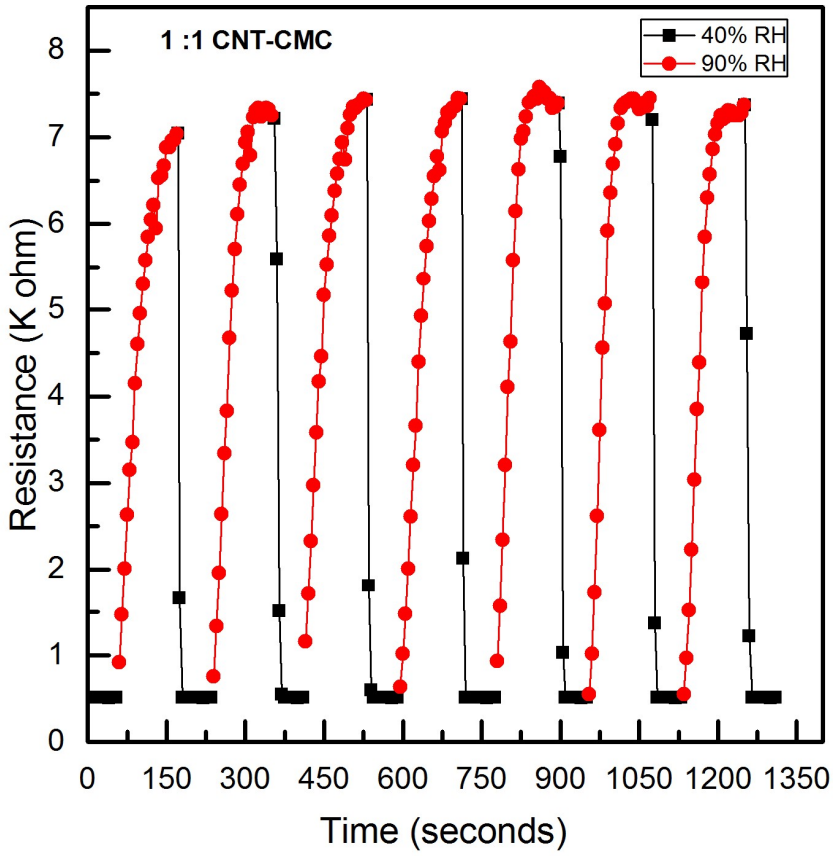


Figure 16. Humidity sensing results from 1:1 CNT-CMC ratio based composite ink.

The performance of the humidity sensors was also found to depend on the CMC and CNT ratio in the composite. We evaluated various CNT-CMC ratios 1:1, 1:2 and 2:1. It was found that 1:1 of CNT-CMC ratio gave the largest sensitivity. The test was conducted by varying humidity between 35% RH and 90% RH.

## 3.3 Application on Respiratory Rate Monitoring

The humidity sensor was applied to monitor human respiratory rate. The sensor was attached on the inner side of a face mask (Surgical grade fiberglass-free ear loop face mask from Walgreens) to capture the humidity change induced by breathing. Fig. 22 shows the picture of a sensor attached within the face mask. The respiratory rate monitoring was tested by multiple volunteers. The real-time sensing result in Fig. 20 shows that the sensor was able to resolve the pace, speed, and strength of breathing. The sensor was also tested for intermittent forceful and normal breathing. Fig. 20, 21 are the respiratory rate data collected on two different volunteers. While Fig. 20 tested for intermitted heavy and normal breathing, Fig. 21 also shows the consistent breathing result.

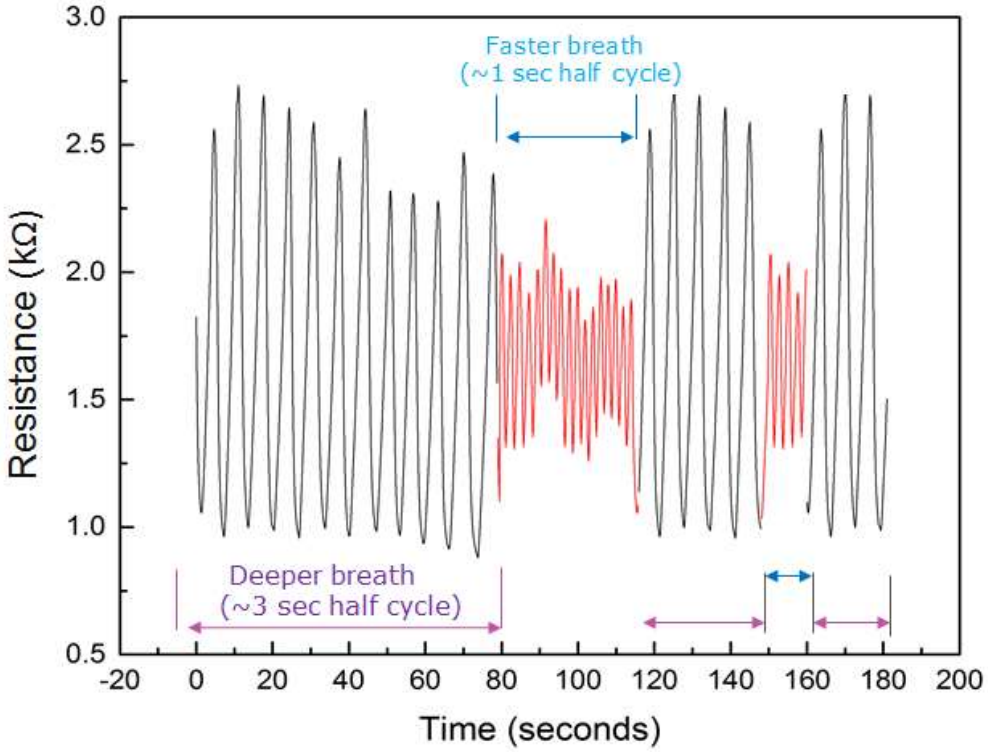


Figure 16. Real-time respiratory rate monitoring.

4. RFID Integration

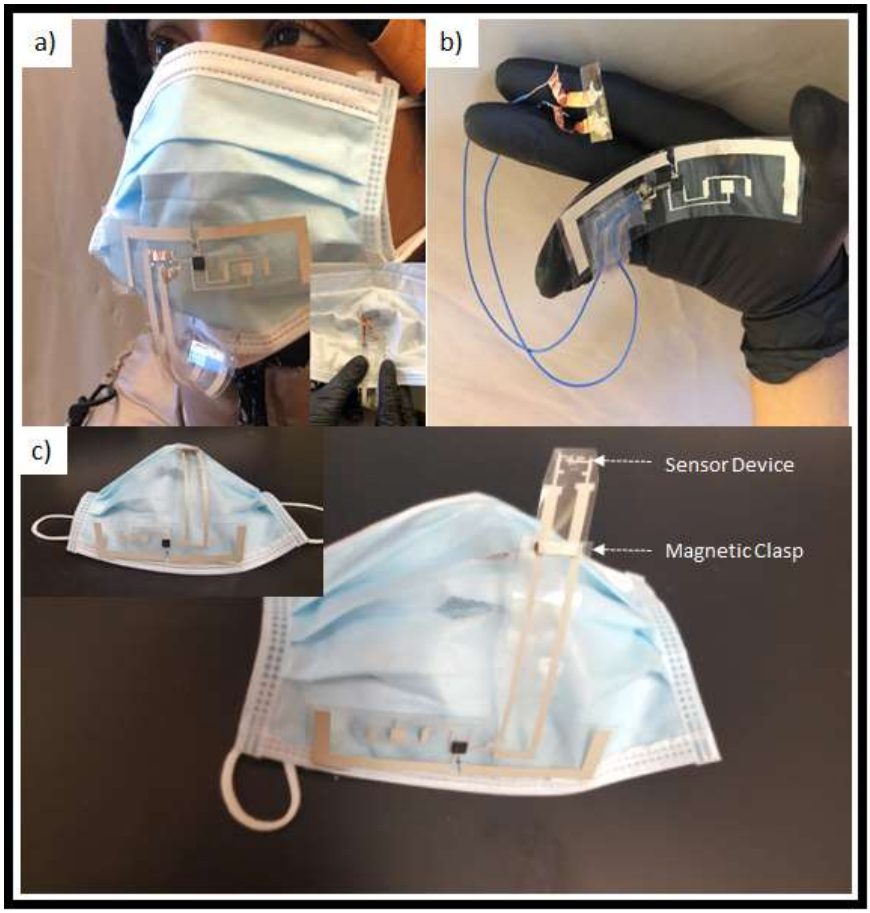


Figure 17. Printed RFID-enabled humidity sensor integrated on a face mask for real-time respiratory rate monitoring. (a) With inset of the interior of the mask. (b) Displays flexibility of the integrated sensor. (c) Optimized integrated sensor.

RFID integration is prominent in customizing the printed electronics to wearable devices. The sensor is currently being attempted to be integrated with active UHF RFID based on an AMS SL900a IC. If succeeded, this achieves the intension of wireless real-time data logging and monitoring.

## 5. Conclusions and Future Work

We have demonstrated sensitive, high-responsive humidity sensor manufactured by using screen printed nanocomposite ink. The nanocomposite material based on CNT, CMC, and PEDOT:PSS forms a CNT-embedded polymer that provides resistance change in response to the adsorption and desorption of moisture. The printed humidity sensor exhibits reliable sensitivity and responsivity in the breathing humidity range. Screen printing the sensor on the flexible PET allowed the possibility of integration on a face mask. Having successfully shown the results of the sensor pacing along with the pace of the breath of different people, the technology may lead to the point-of-care tools capable of improving the diagnosis of sleep disorder or respiratory-related diseases. The future work includes the integration of the sensor with the printed RFID onto wearable devices.

## 6. References


1. Stephan, K., *The OE-A roadmap for organic and printed electronics: creating a guidepost to complex interlinked technologies, applications and markets.* Translational Materials Research, 2016. **3**(1): p. 010301.
2. Mohammed, M.G. and R. Kramer, *All-Printed Flexible and Stretchable Electronics.* Advanced Materials, Δ. **29**(19): p. 1604965.
3. Chen, K., et al., *Printed Carbon Nanotube Electronics and Sensor Systems.* Advanced Materials, 2016. **28**(22): p. 4397-4414.
4. Gaspar, C., et al., *Paper as Active Layer in Inkjet-Printed Capacitive Humidity Sensors.* Sensors (Basel, Switzerland), 2017. **17**(7): p. 1464.
5. Barmpakos, D., et al., *A disposable flexible humidity sensor directly printed on paper for medical applications.* Journal of Physics: Conference Series, 2017. **931**: p. 012003.
6. Dubourg, G., et al., *Fabrication and Characterization of Flexible and Miniaturized Humidity Sensors Using Screen-Printed TiO(2) Nanoparticles as Sensitive Layer.* Sensors (Basel), 2017. **17**(8).
7. Barras, R., et al., *Printable cellulose-based electroconductive composites for sensing elements in paper electronics.* Flexible and Printed Electronics, 2017. **2**(1): p. 014006.
8. Benchirouf, A., et al., *Electrical properties of multi-walled carbon nanotubes/PEDOT:PSS nanocomposites thin films under temperature and humidity effects.* Sensors and Actuators B: Chemical, 2016. **224**: p. 344-350.
9. Xuan, W., et al., *High sensitivity flexible Lamb-wave humidity sensors with a graphene oxide sensing layer.* Nanoscale, 2015. **7**(16): p. 7430-6.
10. Jalkanen, T., et al., *Fabrication of Porous Silicon Based Humidity Sensing Elements on Paper.* Journal of Sensors, 2015. **2015**: p. 10.
11. Li, Y., T. Wu, and M. Yang, *Humidity sensors based on the composite of multi-walled carbon nanotubes and crosslinked polyelectrolyte with good sensitivity and capability of detecting low humidity.* Sensors and Actuators B: Chemical, 2014. **203**: p. 63-70.
12. Mraović, M., et al., *Humidity sensors printed on recycled paper and cardboard.* Sensors (Basel, Switzerland), 2014. **14**(8): p. 13628-13643.
13. Kulkarni, M.V., et al., *Ink-jet printed conducting polyaniline based flexible humidity sensor.* Sensors and Actuators B: Chemical, 2013. **178**: p. 140-143.
14. Weremczuk, J., G. Tarapata, and R. Jachowicz, *Humidity Sensor Printed on Textile with Use of Ink-Jet Technology.* Procedia Engineering, 2012. **47**: p. 1366-1369.
15. Han, J.-W., et al., *Carbon Nanotube Based Humidity Sensor on Cellulose Paper.* The Journal of Physical Chemistry C, 2012. **116**(41): p. 22094-22097.
16. Karimov, K.S., et al., *Humidity Sensing Properties of Carbon Nano-Tube Thin Films.* Sensor Letters, 2011. **9**(5): p. 1649-1653.
17. Cao, C.L., et al., *Humidity Sensor Based on Multi-Walled Carbon Nanotube Thin Films.* Journal of Nanomaterials, 2011. **2011**: p. 1-5.
18. Virtanen, J., et al., *Inkjet-Printed Humidity Sensor for Passive UHF RFID Systems.* IEEE Transactions on Instrumentation and Measurement, 2011. **60**(8): p. 2768-2777.
19. Reddy, A.S.G., et al., *Fully Printed Flexible Humidity Sensor.* Procedia Engineering, 2011. **25**: p. 120-123.
20. Yoo, K.-P., et al., *Novel resistive-type humidity sensor based on multiwall carbon nanotube/polyimide composite films.* Sensors and Actuators B: Chemical, 2010. **145**(1): p. 120-125.
21. Yeow, J.T.W. and J.P.M. She, *Carbon nanotube-enhanced capillary condensation for a capacitive humidity sensor.* Nanotechnology, 2006. **17**(21): p. 5441-5448.

22. Jiang, W.F., et al., *Resistive humidity sensitivity of arrayed multi-wall carbon nanotube nests grown on arrayed nanoporous silicon pillars.* Sensors and Actuators B: Chemical, 2007. **125**(2): p. 651-655.
23. Ribeiro, B., et al., *Carbon nanotube buckypaper reinforced polymer composites: A review*. Vol. 27. 2017.
24. Lu, W., et al., *State of the Art of Carbon Nanotube Fibers: Opportunities and Challenges.* Advanced Materials, 2012. **24**(14): p. 1805-1833.
25. Zahab, A., et al., *Water-vapor effect on the electrical conductivity of a single-walled carbon nanotube mat*. Vol. 62. 2000. 65536-10003.
26. Adjizian, J.-J., et al., *Boron- and nitrogen-doped multi-wall carbon nanotubes for gas detection.* Carbon, 2014. **66**: p. 662-673.
27. Yu, H., et al., *Layer-by-Layer assembly and humidity sensitive behavior of poly(ethyleneimine)/multiwall carbon nanotube composite films.* Sensors and Actuators B: Chemical, 2006. **119**(2): p. 512-515.
28. Liu, S., M. Hu, and J. Yang, *A facile way of fabricating a flexible and conductive cotton fabric.* Journal of Materials Chemistry C, 2016. **4**(6): p. 1320-1325.
29. Lekpittaya, P., et al., *Resistivity of conductive polymer–coated fabric.* Journal of Applied Polymer Science, 2004. **92**(4): p. 2629-2636.
30. Vuorinen, T., et al., *Inkjet-Printed Graphene/PEDOT:PSS Temperature Sensors on a Skin-Conformable Polyurethane Substrate.* Scientific reports, 2016. **6**: p. 35289-35289.
31. Patil, S., et al., *PVA modified ZnO nanowire based microsensors platform for relative humidity and soil moisture measurement.* Sensors and Actuators B: Chemical, 2017. **253**: p. 1071-1078.
32. Shen, W., et al., *Preparation of solid silver nanoparticles for inkjet printed flexible electronics with high conductivity.* Nanoscale, 2014. **6**(3): p. 1622-8.
33. Maiaugree, W., et al., *Influence of Acid Modification Multiwall Carbon Nanotube Counter Electrodes on the Glass and Flexible Dye-Sensitized Solar Cell Performance.* International Journal of Photoenergy, 2016. **2016**: p. 10.
34. Hecht, D.S., L. Hu, and G. Grüner, *Electronic properties of carbon nanotube/fabric composites.* Current Applied Physics, 2007. **7**(1): p. 60-63.
35. Zaporotskova, I.V., et al., *Carbon nanotubes: Sensor properties. A review.* Modern Electronic Materials, 2016. **2**(4): p. 95-105.
36. Kamyshny, A. and S. Magdassi, *Conductive Nanomaterials for Printed Electronics.* Small, 2014. **10**(17): p. 3515-3535.
37. Chen, B., et al., *Fully Packaged Carbon Nanotube Supercapacitors by Direct Ink Writing on Flexible Substrates.* ACS Applied Materials & Interfaces, 2017. **9**(34): p. 28433-28440.
38. Zhang, Y., J.J. Magan, and W.J. Blau, *A general strategy for hybrid thin film fabrication and transfer onto arbitrary substrates.* Sci Rep, 2014. **4**: p. 4822.
39. Menon, H., R. Aiswarya, and K.P. Surendran, *Screen printable MWCNT inks for printed electronics.* RSC Advances, 2017. **7**(70): p. 44076-44081.
40. Ghahremani Honarvar, M. and M. Latifi, *Overview of wearable electronics and smart textiles.* The Journal of The Textile Institute, 2016. **108**(4): p. 631-652.
41. Stoppa, M. and A. Chiolerio, *Wearable Electronics and Smart Textiles: A Critical Review.* Sensors, 2014. **14**(7).

Kazani, I., Hertleer, C., De Mey, G., Schwarz, A., Guxho, G., & Van Langenhove, L. (2012). *Electrical conductive textiles obtained by screen printing.* Fibres & Textiles in Eastern Europe, *20*(1), 57–63.

44. C. Moraes, Galeazzo, E.M. Peres, and J.Fernandez, *Development of Fast Response Humidity Sensors Based on Carbon Nanotubes,* SensorDevices2014. ISBN: 978-1-61208-375-9
45. Benchirouf, A., et al., *Electrical properties of multi-walled carbon nanotubes/PEDOT:PSS nanocomposites thin films under temperature and humidity effects.* Sensors and Actuators B: Chemical, 2016. **224**: p. 344-350.

46. Karimov, K.S., et al., *Humidity Sensing Properties of Carbon Nano-Tube Thin Films.* Sensor Letters, 2011. **9**(5): p. 1649-1653.
47. Han, J.-W., et al., *Carbon Nanotube Based Humidity Sensor on Cellulose Paper.* The Journal of Physical Chemistry C, 2012. **116**(41): p. 22094-22097.
48. https://www.vimbly.com/chicago/dan-macdonald-studios/diy-screen-printing-workshop
49. https://ams.com/sl900a-demokit